

# NJC

Accepted Manuscript



This is an *Accepted Manuscript*, which has been through the Royal Society of Chemistry peer review process and has been accepted for publication.

*Accepted Manuscripts* are published online shortly after acceptance, before technical editing, formatting and proof reading. Using this free service, authors can make their results available to the community, in citable form, before we publish the edited article. We will replace this *Accepted Manuscript* with the edited and formatted *Advance Article* as soon as it is available.

You can find more information about *Accepted Manuscripts* in the [Information for Authors](#).

Please note that technical editing may introduce minor changes to the text and/or graphics, which may alter content. The journal's standard [Terms & Conditions](#) and the [Ethical guidelines](#) still apply. In no event shall the Royal Society of Chemistry be held responsible for any errors or omissions in this *Accepted Manuscript* or any consequences arising from the use of any information it contains.

## ARTICLE

# DNA Stabilized Silver Nanoclusters as the Fluorescence Probe for Studying the Structural Fluctuations and the Solvation Dynamics of the Human Telomeric DNA

Cite this: DOI: 10.1039/x0xx00000x

Received 00th January 2012,  
Accepted 00th January 2012

DOI: 10.1039/x0xx00000x

www.rsc.org/

Hung-Chi Hsu<sup>a</sup>, Meng-Chieh Ho<sup>a</sup>, Kai-Hung Wang<sup>a</sup>, Ying-Feng Hsu<sup>a</sup>, and Chih-Wei Chang<sup>\*,a</sup>

We have prepared the fluorescent silver nanoclusters (AgNCs) in the human telomeric sequence (d[AG<sub>3</sub>(T<sub>2</sub>AG<sub>3</sub>)<sub>3</sub>], Hum 22). There are two types of AgNCs that can be formed in the Hum 22. The red emissive AgNCs ( $\lambda_{em}=620$  nm) are originated from the AgNCs attached on guanine bases, while the green emissive AgNCs ( $\lambda_{em}=520$  nm) are due to the AgNCs located between the adenine and guanine bases. We found that the fluorescence of the AgNCs will be significantly quenched when the Hum 22 forms G-quadruplex structure. The fluorescence anisotropy decay dynamics and the time-resolved emission spectra of the AgNCs reveal the structural fluctuation and the solvation dynamics of the Hum 22. The results indicate that the silver nanoclusters are ideal fluorescence probe for human telomeric DNA and might be an important tool for studying the G-quadruplex structure.

## Introduction

Recently, the silver nanoclusters (AgNCs) have received considerable attention due to their remarkable optical properties and potential applications in many fields.<sup>1-4</sup> The AgNCs can be synthesized by chemical or photo-reduction of the silver salts. In order to avoid forming larger nanoparticles, the AgNCs need to be prepared in different stabilizing scaffolds (such as: dendrimers,<sup>5</sup> polymers,<sup>6-8</sup> proteins<sup>9</sup> and DNAs<sup>2</sup>). In contrast to the large silver nanoparticles, the AgNCs only containing tens to hundreds of silver atoms, and the energy level of the AgNCs is discrete as a result of insufficient atoms to maintain the continuous band structure.<sup>1</sup> As a fluorescence probe, the AgNCs are superior to organic dye and inorganic quantum dots in many aspects. The small size of the AgNCs can minimize the steric hindrance; hence, the AgNCs are ideal fluorescent reporters for the biomolecules as they are sensitive to the steric hindrance caused by the external chromophore. The AgNCs are photostable, nontoxic and highly emissive. These unique features make them suitable for the bio-image or single molecule studies. Furthermore, recent studies have demonstrated a variety of applications of the AgNCs in the detection of metal ions,<sup>10, 11</sup> DNAs<sup>12</sup>, MicroRNAs<sup>13</sup>, and drug-DNA interactions.<sup>14</sup>

Among the templates being utilized to prepare the AgNCs, the DNA oligonucleotides have received special attention, because the emission wavelengths of the DNA:AgNCs complexes (DNA-AgNCs) can be easily tuned from visible to near infrared regions.<sup>15-17</sup> In the past few years, the origin of the colors of the DNA-AgNCs has been extensively investigated.<sup>17-23</sup> The results indicated that the spectral properties of the AgNCs are controlled by multiple factors, such as the number of silver atoms<sup>22</sup>; the shape<sup>21</sup> and the oxidation states<sup>19, 24</sup> of the AgNCs; the conformation of deoxyribose<sup>25</sup>; flexibility of backbone<sup>26</sup> and the silver-base interactions.<sup>17</sup> The quantum chemical calculation suggested that the AgNCs prefer to bind on the doubly bonded ring nitrogen of the bases, and each cluster might simultaneously bind to multiple bases in DNA strands.<sup>27</sup> In 2014, Gwinn and his team demonstrated that the emission of the AgNCs in the DNA templates showed a bimodal distribution with the green emissive AgNCs near 540 nm and the red emissive AgNCs near 630 nm.<sup>22</sup> In their studies, the green and red emitters are attributed to the AgNCs composed of four and six silver atoms, respectively. Meanwhile, many efforts have been devoted to investigating the photophysics of the DNA:AgNCs.<sup>28-30</sup> The solvatochromic study suggested that the AgNCs exhibit large dipole moment changes upon excitation,<sup>31</sup> and the excited DNA-AgNCs return to the ground state through the radiative state and the long-live dark

charge-transfer(CT) state.<sup>2, 28, 30</sup> The fluorescence lifetime of DNA-AgNCs is about 2~3 ns,<sup>19, 29</sup> while recombination of the CT state occurred in  $\mu$ s time scale.<sup>28</sup>

In contrast to the studies using X-ray, NMR and circular dichroism (CD) spectroscopies, the fluorescence spectroscopy is highly sensitive and providing superior time resolution that can be utilized to monitor the dynamical structural fluctuations in real time. Because the DNA bases only exhibit weak intrinsic fluorescence, the application of fluorescence method in DNA study usually required the labelling of external chromophore, which requires complex labelling process and might significantly perturb the structure.<sup>32</sup> To avoid this problem, we have employed the AgNCs as the fluorescence probe to investigate the structural dynamics of the human telomeric sequence (d[AG<sub>3</sub>(T<sub>2</sub>AG<sub>3</sub>)<sub>3</sub>], Hum 22). For many years, the Hum 22 was utilized as the model system for studying the structural polymorphism of G-rich quadruplex.<sup>33</sup> Although the G-quadruplex templated AgNCs have been employed in bio-image study,<sup>34</sup> the understanding about the photophysics and the spectral heterogeneity of the AgNCs on G-quadruplex template are still far from complete. In this study, optical properties of the AgNCs synthesized in Hum 22 template will be addressed in detail. The information we provide is important for applying the fluorescence method in DNA study. Meanwhile we also demonstrated the feasibility of using the AgNCs as the fluorescence probe to study the dynamical fluctuation and the solvation dynamics of the Hum 22.

## Experimental

### Materials and Preparation of the DNA:AgNCs Complexes

The human telomere sequence (5'-AG<sub>3</sub>(T<sub>2</sub>AG<sub>3</sub>)<sub>3</sub>, Hum 22, HPLC purified) was purchased from the Sigma Aldrich. The desalted dG<sub>12</sub>, dA<sub>12</sub>, dT<sub>12</sub>, d(AG)<sub>11</sub> and d(GT)<sub>11</sub> sequences were purchased from the Integrated DNA Technologies and were used without further purification. The AgNO<sub>3</sub> (>99%), NaBH<sub>4</sub> (>99%) and NaNO<sub>3</sub> (>99%) were also purchased from the Sigma Aldrich and used as received. The deionized water (resistivity>18.2 M $\Omega$ -cm at 25 $^{\circ}$ C) was obtained from the Barnstead™ EasyPure™ II water purification system (Thermo Scientific™) and was used in all experiments. The DNA was firstly dissolved in the deionized water, and the single strand concentration of the DNA was estimated based on the absorbance at 260 nm. After determining the DNA concentration, 30  $\mu$ M of DNA was heated to 90 $^{\circ}$ C for 10 minutes and then slowly cooled down to the room temperature. The DNA-AgNCs were formed by mixing 500  $\mu$ L of DNA (30 $\mu$ M) with 45  $\mu$ L of AgNO<sub>3</sub> (2 mM), and reducing with 45  $\mu$ L of NaBH<sub>4</sub> (2 mM). After mixing with NaBH<sub>4</sub>, the samples were stored at the 4 $^{\circ}$ C refrigerator for at least 12 hours, and diluted to the desired concentration before being used.

### The CD Spectroscopy Measurements

The CD spectra were obtained with a 1  $\times$  1 cm quartz cuvette using Jasco J-810 spectropolarimeter (JASCO, Japan). The sample concentration was 2 $\mu$ M, and the temperature was

controlled at 25 $^{\circ}$ C, using the temperature accessory (JASCO, PTC-423S). The spectra were recorded from 220 to 350 nm at a scanning rate of 100 nm/min. Each spectrum was scanned three times and the background CD spectrum was subtracted.

### Steady State and Time-Resolved Fluorescence Measurements

A 10  $\times$  3 mm quartz cuvette was used for all fluorescence measurements. The steady state emission and the excitation spectra of the AgNCs were recorded by the Cary Eclipse fluorescence spectrophotometer. The time-resolved spectra were acquired using time-correlated photon counting system and the details were described elsewhere.<sup>35</sup> The 445 nm excitation light source was provided by a vertical polarized picosecond-pulsed diode laser (LDH-440, Picoquant). The 550 nm light source was provided by a subnanosecond pulsed LED (PLS 500, Picoquant) in combination with a polarizer and the 550 nm band pass filter (FB550-10, Thorlabs). The polarization of the emission light was selected by a polarizer and the angle of the polarizer was set at 54.7 $^{\circ}$  relative to the polarization of excitation light source.

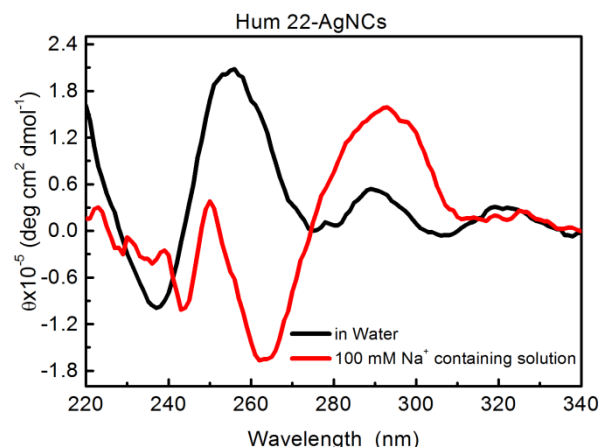


Figure 1: The CD spectra of the Hum 22-AgNCs in water and 100 mM Na<sup>+</sup> containing solution

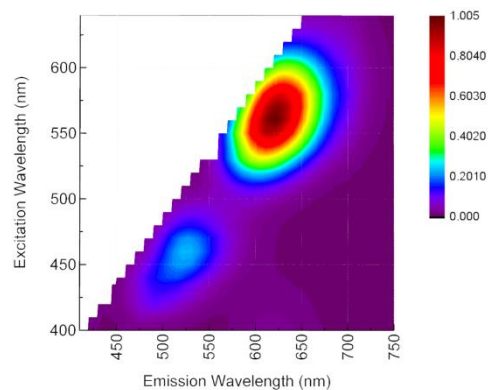


Figure 2: The fluorescence contour map of the Hum 22-AgNCs in water

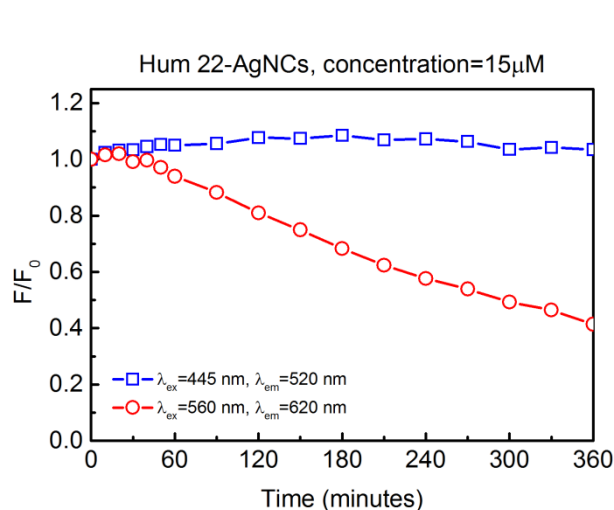


Figure 3: The time-dependence of the fluorescence intensity of the green emissive (blue) and the red emissive (red) AgNCs.

## Results and Discussion

In this study, the AgNCs was prepared via the chemical reduction methods. The Hum 22 sequence was firstly mixed with the  $\text{AgNO}_3$  and then reduced by the  $\text{NaBH}_4$ . Figure 1 shows the circular dichroism (CD) spectra of the Hum 22-AgNCs. The positive band at  $\sim 256$  nm and the negative band at  $\sim 238$  nm indicate the formation of parallel tetramolecular G-quadruplex in the solution.<sup>33</sup> It should be noted that the CD signal of the Hum 22-AgNCs was significantly lower than that of the unmodified Hum 22.<sup>33</sup> The previous studies showed that the  $\text{Ag}^+$  ion is chelating at the N7 and O6 groups in guanine bases; hence, adding the  $\text{Ag}^+$  ion in the solution will inhibit the formation of G-quadruplex in the solution.<sup>18, 27, 36, 37</sup> For this reason, the AgNCs should primary associate with the single-stranded Hum 22. The fluorescence contour map (figure 2) of the Hum 22-AgNCs is featured by two bands: one is central at  $\lambda_{\text{excitation}}/\lambda_{\text{emission}}=460$  nm/520 nm, and the other is central at  $\lambda_{\text{excitation}}/\lambda_{\text{emission}}=560$  nm/620 nm. These two emission bands show distinct excitation spectra (figure S<sub>1</sub>) in the visible region, which suggested that they originated from different emissive species. The excitation spectra in the UV region is the consequence of the energy transfer from the DNA bases to the AgNCs.<sup>16</sup> Figure 3 shows the time-dependence of the fluorescence intensity of Hum 22-AgNCs in the solution. As depicted, the fluorescence intensity of the red emissive AgNCs decrease significantly in the first six hours, but the fluorescence of the green emissive AgNCs only slight increases during the same period. This finding is aligned with the previous studies, in which the green emissive and the red emissive AgNCs are attributed to the oxidized AgNCs and the fully reduced AgNCs, respectively.<sup>24</sup> In contrast to the drastic fluorescence quenching of the red emissive AgNCs, the moderate fluorescence enhancement of the green emissive AgNCs implies that the oxidized AgNCs

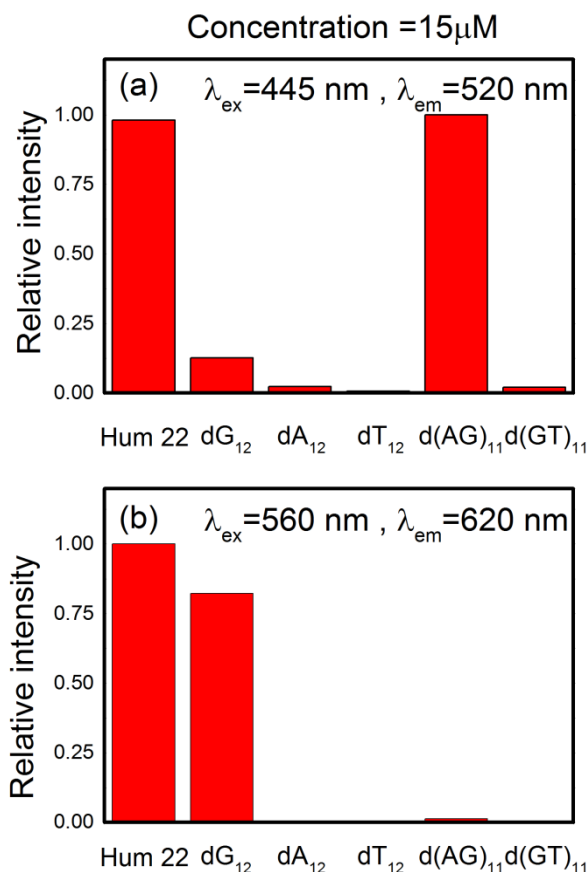


Figure 4: The relative fluorescence intensity of (a) the green emissive and (b) the red emissive AgNCs prepared in different DNA templates.

might have lower fluorescence quantum yield or the oxidation of AgNCs will also generate non-fluorescent AgNCs. As the Hum22 are composed of dG, dA and dT nucleotides, we prepared the AgNCs in the dA<sub>12</sub>, the dT<sub>12</sub>, and the dG<sub>12</sub> sequences. Among these templates, only the dG<sub>12</sub>-AgNCs shows intense fluorescence upon the 560 nm excitation (figure 4b). The result indicates that the red emissive AgNCs are primarily attached to the guanine bases. Although fluorescence intensity of the dG<sub>12</sub>-AgNCs at 620 nm is comparable with that of the Hum 22-AgNCs, the dG<sub>12</sub>-AgNCs only shows weak emission at 520 nm upon the 445 nm excitation (figure 4a). This finding suggests that the fluorescent oxidized AgNCs need to be stabilized by at least two different kinds of bases. To address the concern of this issue, we also employed d(AG)<sub>11</sub> and d(GT)<sub>11</sub> as templates. As depicted, only the d(AG)<sub>11</sub>-AgNCs shows strong fluorescence upon 445 nm excitation (figure 4a). These evidences supported that the adenine is crucial for stabilizing the green emissive AgNCs, and the green emissive AgNCs are located in between the dA and dG bases.

It has been well documented that certain monovalent cations ( $\text{Na}^+$  or  $\text{K}^+$ ) can significantly improve the stability of the G-quadruplex structure in the solution.<sup>38</sup> To collect more information about the optical properties of the AgNCs in different DNA secondary structures, we performed the  $\text{Na}^+$  ion

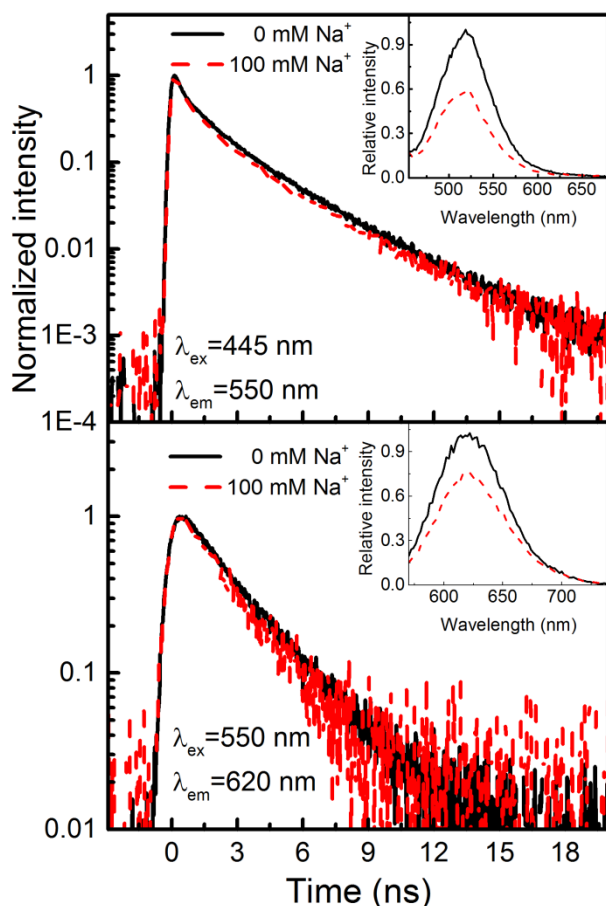


Figure 5: The time-resolved fluorescence decays of: (upper) the green emissive AgNCs (upper) and the red emissive AgNCs (lower) in different  $\text{Na}^+$  ion concentrations. The corresponding steady state emission spectra are presented in the inset

titration experiment for the Hum 22-AgNCs. Because the chloride ion might interact with the oxidized nanocluster,<sup>19</sup> we used the sodium nitrate salt rather than sodium chloride salt in our study. In the  $\text{Na}^+$  containing solution, the CD spectrum of the Hum 22-AgNCs shows the typical signature of an antiparallel intramolecular G-quadruplex (figure 1).<sup>38</sup> Meanwhile, both the green and red emission bands of the Hum 22-AgNCs are drastically quenched (figure 5, inset). The fluorescence lifetime measurement indicates that the presence of the  $\text{Na}^+$  ion only shows a little effect on the fluorescence decay of the AgNCs (figure 5). Therefore, the fluorescence quenching is mainly through the static quenching mechanism. The controlled experiment shows that the  $\text{Na}^+$  ion does not quench the fluorescence of the AgNCs synthesized in the poly (methacrylic acid) solution (figure S<sub>2</sub>); which also supports that the fluorescence quenching is not due to the collisional quenching of the  $\text{Na}^+$  ion. These evidences suggest that the fluorescence quenching of the Hum 22-AgNCs in  $\text{Na}^+$  solution is caused by the formation of the antiparallel G-quadruplex in the solution. It should be noted that the fluorescence of the

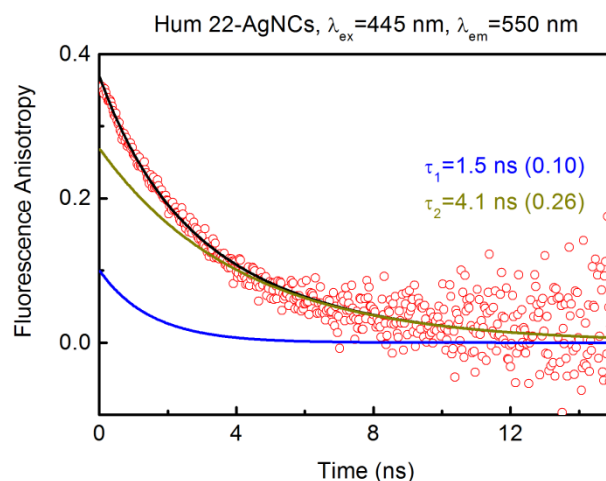


Figure 6: The time-resolved anisotropy decay of the Hum 22-AgNCs

Hum 22-AgNCs can be recovered after removing the  $\text{Na}^+$  ion by ultrafiltration tube (Microsep<sup>TM</sup>, MWCO=3000, PALL) (Figure S<sub>3</sub>). Therefore, the AgNCs must remain attached on the Hum 22 when forming G-quadruplex. Since the red emissive AgNCs is primarily located at the guanine bases, the fluorescence quenching we observed is associated with the formation of Hoogsteen hydrogen bond networks in the G-quadruplex, and similar fluorescence quenching was also observed when probing the intrinsic fluorescence of G-rich sequence.<sup>39</sup>

Although the time-resolution of our instrument cannot resolve the initial ultrafast decay component of the AgNCs,<sup>40</sup> the Hum 22-AgNCs still reveals several interesting dynamics in the nanosecond time scale. In the biophysical study, the fluorescence anisotropy measurement is normally used to interpret the hydrodynamic radius and the local flexibility of the biomolecules in the solution. For the chromophore that is bound to a macromolecule and undergoes segmental motions, the fluorescence anisotropy dynamics “ $r(t)$ ” is given by<sup>41</sup>:

$$r(t) = r_0(f_S e^{-t/\theta_S} + f_L e^{-t/\theta_L}) \quad (1)$$

the subscripts S and L refer to the short and long correlation time. The correlation time for the segmental motions ( $\theta_{\text{seg}}$ ) and the overall rotation of the macromolecule ( $\theta_{\text{rot}}$ ) can be represented as<sup>41</sup>:

$$\frac{1}{\theta_S} = \frac{1}{\theta_{\text{seg}}} + \frac{1}{\theta_{\text{rot}}}, \quad \frac{1}{\theta_L} = \frac{1}{\theta_{\text{rot}}} \quad (2)$$

The hydrodynamic molecular volume (V) for spherical molecular can be estimated using the Perrin’s equation:

$$\theta_{\text{rot}} = \frac{V\eta}{RT} \quad (3)$$

Here  $\eta$  is the viscosity of the medium ( $\eta=0.8937$  mPa·s at 298K), T is the temperature, and R is the gas constant. The



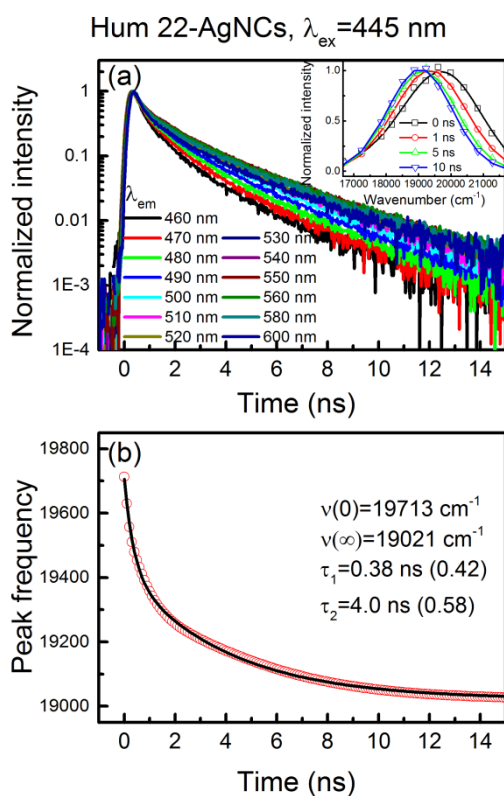


Figure 7: (a) The fluorescence decays and the TRES of the green emissive AgNCs. (b) The spectral relaxation dynamics of the green emissive AgNCs, the relative amplitude of each component was indicated in the parenthesis.

anisotropy decay dynamics of the Hum 22-AgNCs shows a bi-exponential decay with time-coefficients of 1.5 and 4.1 ns (figure 6). According to equation (2),  $\theta_{seg}$  is estimated to be 2.37 ns, while the 4.1 ns rotational correlation time corresponds to the hydrodynamics radius  $\sim 1.65$  nm.

Another interesting finding is the spectral relaxation dynamics of the Hum22-AgNCs. Upon the 550 nm excitation, the fluorescence decays of the AgNCs are independent of the emission wavelengths and show a bi-exponential decay with time coefficients of 0.85 ns and 2.82 ns (figure S4). However, the transients excited at 445 nm revealed a clear wavelength dependent feature, and the fluorescence decays gradually slow down toward longer emission wavelengths (figure 7a). The result implies that the emission spectra for the green emissive AgNCs are also time-dependent. To address the concern of this issue, the time-resolved emission spectra (TRES) are constructed based on the method proposed by Maroncelli and Fleming.<sup>42</sup> As depicted (figure 7a, inset), the TRES show the clear relaxation dynamics in the nanosecond time scale. The spectral relaxation dynamics can be fitted by a bi-exponential decay with time coefficients of 0.38 ns and 4 ns. (Figure 7b) The observing dynamics could be the result of either solvation or the emission from multiple emissive species.<sup>35, 41</sup> In order to verify the origin of the spectra relaxation dynamics we observed, we measured the spectra relaxation dynamics of the Hum22-AgNCs in polyvinyl alcohol (PVA) film (figure S<sub>5</sub>), in which the spectra relaxation dynamics caused by solvation are

completely inhibited. In the PVA film, the TRES of the Hum 22-AgNCs also show the relaxation dynamics in the nanosecond time scale, but, the relaxation energy is significantly decreased. The result shows that the large time-dependent Stokes shift we observed in the solution reflects the solvation dynamics near the DNA bases, which aligns with the prior solvation studies using base stacked coumarin.<sup>43, 44</sup>

## Conclusions

In this study, we employed the fluorescent silver nanoclusters as the fluorescence probe for the human telomeric DNA. The result shows that the Hum 22-silver nanoclusters are composed of the green emissive silver nanoclusters ( $\lambda_{excitation}/\lambda_{emission} = 460$  nm/520 nm) and the red emissive silver nanoclusters ( $\lambda_{excitation}/\lambda_{emission} = 560$  nm/620 nm). By preparing the silver nanoclusters in different DNA templates, we found that the red emissive silver nanoclusters are primarily associated with the guanine base, whereas the green emissive silver nanoclusters are located between the adenine and guanine bases. In the  $\text{Na}^+$  containing solution, fluorescence of the Hum 22-silver nanoclusters is significantly quenched due to the formation of the anti-parallel G-quadruplex. The fluorescence anisotropy decay of the Hum 22-silver nanoclusters was featured by a bi-exponential decay with time-coefficients of 1.5 ns and 4.1 ns. The fast component refers to the fast wobbling motion of the DNA bases, while the slow decay component is attributed to the rotation of Hum22-silver nanoclusters. The hydrodynamics radius of the Hum 22-silver nanoclusters is estimated to be about 1.65 nm. Upon the 445 nm excitation, the green emissive silver nanoclusters exhibit the clear spectra relaxation dynamics in the nanosecond time scale. The nanosecond solvation dynamics we observed aligns with the solvation studies using base stacked coumarin, and our finding reveals the potential applications of the silver nanoclusters in DNA solvation studies.

In summary, by performing complete analysis for the optical properties and the excited state dynamics of the Hum 22-silver nanoclusters, we have demonstrated the feasibility of using silver nanoclusters as the fluorescence probe in human telomeric DNA. Fluorescence spectroscopy provides a highly sensitive method for studying the structural fluctuations of the G-quadruplex in real time. The information we provided is not only important for understanding the photophysics of the silver nanoclusters on DNA, but also essential for the application of the fluorescence method in studying the structural dynamics of various DNA secondary structures.

## Acknowledgements

We sincerely appreciate the support from the Ministry of Science and Technology of Taiwan (Project contracts: NSC 102-2113-M-018-005-MY2). We also thank Dr. Yi-Hong Lin (National Synchrotron Radiation Research Center) for his support in the CD experiments, and Ms. Sophie Yun-Chen Wu for her modification in this manuscript.

## Notes and References

<sup>a</sup> Department of Chemistry, National Changhua University of Education, Changhua 50058, Taiwan

Electronic Supplementary Information (ESI) available: [Figure S<sub>1</sub>: the excitation spectra of Hum 22-AgNCs; Figure S<sub>2</sub>: the Na<sup>+</sup> quenching experiment of AgNCs synthesized in polymer scaffold; Figure S<sub>3</sub>: the fluorescence recovery experiment of Hum 22-AgNCs; Figure S<sub>4</sub>: The fluorescence decay of Hum 22-AgNCs upon the 550 nm excitation; Figure S<sub>5</sub>: the fluorescence decay, TRES and spectral relaxation dynamics of Hum 22-AgNCs embedded in polyvinyl alcohol film.]. See DOI: 10.1039/b000000x/

## References

1. I. Díez and R. H. Ras, in *Advanced fluorescence reporters in chemistry and biology II*, Springer Berlin Heidelberg 2010, pp. 307-332.
2. J. T. Petty, S. P. Story, J.-C. Hsiang and R. M. Dickson, *J. Phys. Chem. Lett.*, 2013, **4**, 1148-1155.
3. J. M. Obliosca, C. Liu and H.-C. Yeh, *Nanoscale*, 2013, **5**, 8443-8461.
4. S. Choi, R. M. Dickson and J. Yu, *Chem. Soc. Rev.*, 2012, **41**, 1867-1891.
5. J. Zheng and R. M. Dickson, *J. Am. Chem. Soc.*, 2002, **124**, 13982-13983.
6. J. Zhang, S. Xu and E. Kumacheva, *Adv. Mater.*, 2005, **17**, 2336-2340.
7. Z. Shen, H. Duan and H. Frey, *Adv. Mater.*, 2007, **19**, 349-352.
8. I. Díez, R. H. A. Ras, M. I. Kanyuk and A. P. Demchenko, *Phys. Chem. Chem. Phys.*, 2013, **15**, 979-985.
9. S. S. Narayanan and S. K. Pal, *J. Phys. Chem. C*, 2008, **112**, 4874-4879.
10. Y.-T. Su, G.-Y. Lan, W.-Y. Chen and H.-T. Chang, *Anal. Chem.*, 2010, **82**, 8566-8572.
11. K. S. Park and H. G. Park, *Curr. Opin. Biotechnol.*, 2014, **28**, 17-24.
12. H.-C. Yeh, J. Sharma, J. J. Han, J. S. Martinez and J. H. Werner, *Nano. Lett.*, 2010, **10**, 3106-3110.
13. S. W. Yang and T. Vosch, *Anal. Chem.*, 2011, **83**, 6935-6939.
14. J. Yuan, W. Guo and E. Wang, *Anal. Chim. Acta.*, 2011, **706**, 338-342.
15. C. I. Richards, S. Choi, J.-C. Hsiang, Y. Antoku, T. Vosch, A. Bongiorno, Y.-L. Tzeng and R. M. Dickson, *J. Am. Chem. Soc.*, 2008, **130**, 5038-5039.
16. P. R. O'Neill, E. G. Gwinn and D. K. Fyngenson, *J. Phys. Chem. C*, 2011, **115**, 24061-24066.
17. D. Schultz and E. G. Gwinn, *Chem. Comm.*, 2012, **48**, 5748-5750.
18. B. Sengupta, C. M. Ritchie, J. G. Buckman, K. R. Johnsen, P. M. Goodwin and J. T. Petty, *J. Phys. Chem. C*, 2008, **112**, 18776-18782.
19. J. Sharma, H.-C. Yeh, H. Yoo, J. H. Werner and J. S. Martinez, *Chem. Comm.*, 2010, **46**, 3280-3282.
20. D. Schultz, K. Gardner, S. S. R. Oemrawsingh, N. Markešević, K. Olsson, M. Debord, D. Bouwmeester and E. Gwinn, *Advanced materials*, 2013, **25**, 2797-2803.
21. R. R. Ramazanov and A. I. Kononov, *J. Phys. Chem. C*, 2013, **117**, 18681-18687.
22. S. M. Copp, D. Schultz, S. Swasey, J. Pavlovich, M. Debord, A. Chiu, K. Olsson and E. Gwinn, *J. Phys. Chem. Lett.*, 2014, **5**, 959-963.
23. P. Shah, P. W. Thulstrup, S. K. Cho, Y.-J. Bhang, J. C. Ahn, S. W. Choi, M. J. Bjerrum and S. W. Yang, *Analyst*, 2014, **139**, 2158-2166.
24. C. M. Ritchie, K. R. Johnsen, J. R. Kiser, A. Antoku, R. M. Dickson and J. T. Petty, *J. Phys. Chem. C*, 2007, **111**, 175-181.
25. D. Schultz and E. Gwinn, *ChemComm*, 2011, **47**, 4715-4717.
26. P. Shah, P. W. Thulstrup, S. K. Cho, M. J. Bjerrum and S. W. Yang, *Chem. Comm.*, 2014, **50**, 15392-15395.
27. V. Soto-Verdugo, H. Metiu and E. Gwinn, *J. Chem. Phys.*, 2010, **132**, 195102-195101 -195102-195109.
28. S. A. Patel, M. Cozzuol, J. M. Hales, C. I. Richards, M. Sartin, J.-C. Hsiang, T. Vosch, J. W. Perry and R. M. Dickson, *J. Phys. Chem. C*, 2009, **113**, 20264-20270.
29. S. A. Patel, C. I. Richards, J.-C. Hsiang and R. M. Dickson, *J. Am. Chem. Soc.*, 2008, **130**, 11602-11603.
30. I. L. Volkov, P. Yu, Serdobintsev and A. I. Kononov, *J. Phys. Chem. C*, 2013, **117**, 24079-24083.
31. F. Qu, L. L. Dou, N. B. Li and H. Q. Luo, *J. Mater. Chem. C*, 2013, **1**, 4008-4013.
32. K. E. Furse and S. A. Corcelli, *J. Phys. Chem. B*, 2010, **114**, 9934-9945.
33. M.-C. Ho and C.-W. Chang, *RSC Advance*, 2014, **4**, 20531-20534.
34. J. Ai, W. Guo, B. Li, T. Li, D. Li and E. Wang, *Talanta*, 2012, **88**, 450-455.
35. H.-Y. Weng, K.-M. Lee, Y.-S. Chen and C.-W. Chang, *Phys. Chem. Chem. Phys.*, 2013, **15**, 16935-16940.
36. X.-H. Zhou, D.-M. Kong and H.-X. Shen, *Anal. Chem.*, 2010, **82**, 789-793.
37. H. Arakawa, J. F. Neault and H. A. Tajmir-Riahi, *Biophys. J.*, 2001, **81**, 1580-1587.
38. S. Neidle and S. Balasubramanian, *Quadruplex nucleic acids*, Royal Society of Chemistry, Cambridge, 2006.
39. N. T. Dao, R. Haselsberger, M.-E. Michel-Beyerle and A. T. Phan, *FEBS Lett.*, 2011, **585**, 3969-3977.
40. S. H. Yau, N. Abeyasinghe, M. Orr, L. Upton, O. Varnavski, J. H. Werner, H.-C. Yeh, J. Sharma, A. P. Shreve, J. S. Martinez and T. G. S. III, *nanoscale*, 2012, **4**, 4247-4254.
41. J. R. Lakowicz, *Principle of fluorescence spectroscopy*, Springer 2006.
42. M. Maroncelli and G. R. Fleming, *J. Chem. Phys.*, 1987, **86**, 6221.
43. S. D. Verma, N. Pal, M. K. Singh and S. Sen, *J. Phys. Chem. Lett.*, 2012, **3**, 2621-2626.
44. S. Sen, D. Andreatta, S. Y. Ponomarev, D. L. Beveridge and M. A. Berg, *J. Am. Chem. Soc.*, 2009, **131**, 1724-1735.